

Short Communication

Corrosion Behaviour of Three Kinds of Arc Sprayed Coatings in Soil

Jialiang Song^{1,2}, Zhaoliang Li^{1,2}, Dongjiu Zhang⁴, Qiong Yao⁴, Ziheng Bai^{1,2}, Yali Feng^{1,2},
Chaofang Dong^{1,2} and Kui Xiao^{1,2*}

¹ Corrosion and Protection Center, University of Science and Technology Beijing, Beijing 100083, China.

² National Materials Corrosion and Protection Data Center, University of Science and Technology Beijing, Beijing 100083, China.

³ Key Laboratory of Space Launching Site Reliability Technology, Haikou 571000, China.

*E-mail: xiaokui@ustb.edu.cn

Received: 21 June 2019 / Accepted: 25 August 2019 / Published: 29 October 2019

The corrosion resistance of a pure Zn coating, a ZnAl alloy coating and a ZnAl pseudo-alloy coating in a Beijing area was studied. The corrosion products were analysed by XRD, and the electrochemical processes of the three coatings were analysed by measuring the electrochemical impedance and polarization curves. The results showed that the surface corrosion products of the pure Zn coating were mainly composed of $Zn_5(OH)_8Cl_2H_2O$, $ZnCO_3$, ZnO and $Zn_5(CO_3)_2(OH)_6$, while the surface corrosion products of the ZnAl alloy and ZnAl pseudo-alloy coating similarly consisted of $Zn_5(OH)_8Cl_2H_2O$, $Zn_{0.71}Al_{0.29}(OH)_2(CO_3) \cdot 0.145xH_2O$ and $ZnO \cdot Al_2O_3$. Before and after corrosion, the order of the coating corrosion resistance was as follows: ZnAl alloy coating > ZnAl pseudo-alloy coating > pure Zn coating. It was found that a "self-sealing" protective effect of the ZnAl alloy coating was better than that of the ZnAl pseudo-alloy coating because the composition was more uniformly distributed. The main reason for a weaker "self-sealing" protective effect of the ZnAl pseudo-alloy was that galvanic corrosion occurred between the Zn-rich phase and the Al-rich phase of the pseudo-alloy, which accelerated the electrochemical reaction. Meanwhile, the pure Zn coating did not have the "self-sealing" effect. Consequently, the corrosion resistance of the ZnAl alloy coating was the best.

Keywords: Soil corrosion, Pure Zn coating, ZnAl alloy coating, ZnAl pseudo-alloy coating, Electrochemical test

1. INTRODUCTION

With the development of modern industry, an increasing number of oil, gas and water pipelines are laid underground, usually with high-strength ductile iron [1]; however, they are often corroded to a certain extent. Corrosion in soil is often less noticeable than atmospheric corrosion, so it is expected to

encounter the problem of corrosion in soil on a metal matrix. In modern thermal anti-corrosion spraying technology, arc spraying technology is widely used in anti-corrosion steel structure engineering, and it has excellent performance and high efficiency as well as energy savings, cost savings, the use of simple equipment and other advantages [2,3].

In most environments, the potential of Zn is negative compared with that of steel, which makes it a good material for arc spraying [4] as it conducts a cathodic protection on the substrate. Moreover, when Zn is used as a coating to cover the steel, it can also shield the corrosive medium. With these two important advantages, Zn coating has long been used as an anti-corrosion method for steel [5]. However, a pure Zn coating breaks down quickly in the process of corrosion protection and has a high cost, so it cannot effectively protect the substrate for a long time [5]. Al easily forms a dense oxidation film to protect itself [6], but it is also prone to pitting corrosion [7]. Therefore, after some research on adding Al to a Zn coating, it was found that the combination of Zn [8,9] and Al formed a mesh framework structure in the corrosion process of the coating; this coating hindered the loss of Zn corrosion products and greatly improved the corrosion resistance of the coating by combining the advantages of the two metals [4]. Currently, a ZnAl alloy coating is widely used in anti-corrosion engineering for the long-term protection of steel structures through arc spraying technology. Robert et al. [10] showed that the corrosion resistance of the coating improved with increasing Al content. However, when the proportion of Al in the alloy exceeded 15%, the hardness and brittleness of the material increased significantly, which made it difficult to process the alloy wire. Therefore, to study a ZnAl coating with higher Al content, a ZnAl pseudo-alloy coating appeared whose metallographic structure was composed of a pure Zn phase, a pure Al phase and a few ZnAl alloy phases, which did not belong to the real alloy. Studies [11] showed that the corrosion resistance of a ZnAl pseudo-alloy coating was significantly improved by increasing the Al content.

However, there are relatively few studies and reports on the electrochemical mechanism between thermal spray coatings and corrosion in soil. In addition, the comparative analysis of electrochemical properties between alloys with the same content of Zn and Al and pseudo-alloys is seldom studied. In this paper, 120-day corrosion in soil tests of pure Zn, ZnAl alloy and ZnAl pseudo-alloy arc sprayed coatings were carried out in typical soils of the Shunyi District, Beijing. The composition differences of corrosion products were analysed and compared by X-ray diffraction analysis. The electrochemical impedance spectroscopy (EIS) and polarization curves of samples before and after corrosion were tested. The electrochemical mechanism of corrosion in soil was further analysed, the corrosion resistance of the three coatings was compared, and the reasons for the differences in corrosion resistance were explained.

2. MATERIALS AND METHODS

2.1. Test material

The test selected 10 mm × 10 mm × 10 mm nodular cast iron cube samples, and its surface was sandblasted with 24 mesh corundum sand. The pressure was kept within the range of 50 ~ 60 N. Three coatings of pure Zn, ZnAl alloy and ZnAl pseudo-alloy were prepared by arc spraying. The ZnAl alloy coating used a Φ diameter 3 mm Zn 85%-Al 15% alloy solid core wire for spraying; the ZnAl pseudo-

alloy coating used a Φ 3 mm diameter Zn wire and a Φ 2 mm Al wire for spraying. The coating thickness of the two alloys was approximately 120 μm . The arc spraying process parameters were as follows: current 100~120 A, voltage 36 V, spraying distance 150 mm, and gas pressure 0.6 MPa. Copper wire welding was performed on the back of the coating sample. Epoxy resin was used to seal the 5 surfaces and welding points outside the coating layer, and only a 1 cm^2 effective area was retained.

2.2. Test method

The test soil was taken from typical soil in the Shunyi District of Beijing and sampled at a depth of 1 m. According to the detection by Zhu Min et al. [12], the anion content in the soil was Cl^- 0.25 wt %, SO_4^{2-} 0.1 wt %, CO_3^{2-} 0.05 wt %, and NO_3^- 0.1 wt % along with a water content of 15.88%, and a pH value of 7.64. The coating samples were buried in laboratory containers with a constant indoor temperature of 15°C. Water was sprayed every 10 days to maintain the original soil moisture and the testing length was 120 days.

Electrochemical impedance spectra (EIS) and potentiometric polarization curves of the coated samples after the corrosion in soil test were measured with an EG&G Potentiostat / Galvanostat Mode 1273 electrochemical station. Three-electrode systems were used with the sample as the working electrode, a platinum electrode as the auxiliary electrode and a saturated calomel electrode (SCE) as the reference electrode. The three-electrode system was immersed in 0.5 L of 3.5% NaCl solution to test the open circuit potential, and the electrochemical impedance spectrum and dynamic potential polarization curve were measured after 20 minutes. The frequency range of the electrochemical impedance spectrum was 100,000 Hz ~ 0.01 Hz with an amplitude of 10 mV, a polarization curve scanning rate of 0.6 mV/s, and a scanning range of -0.2 V ~ 0.4 V compared with the open circuit potential. The surface of the remaining parallel samples after the corrosion in soil test was scraped for rust, and a material phase analysis was carried out by using a dmax-rc rotating anode X-ray diffractometer. The radiation source was Cu $K\alpha$, the tube pressure was 40 kV, the current was 150 mA, the scanning range was 10 °~ 100 °, the step width was 0.02 °, and the scanning rate was 10 °·min⁻¹.

3. RESULTS AND DISCUSSION

3.1 XRD analysis of the coating sample surface

Figure 1 shows the X-ray diffraction pattern of the pure Zn, ZnAl alloy and ZnAl pseudo-alloy coating after corrosion in soil for 120 days. The surface corrosion products of the pure Zn coating were mainly composed of $\text{Zn}_5(\text{OH})_8\text{Cl}_2\text{H}_2\text{O}$, ZnCO_3 , ZnO and $\text{Zn}_5(\text{CO}_3)_2(\text{OH})_6$, while the surface corrosion products of the ZnAl alloy and ZnAl pseudo-alloy coating were basically the same and consisted of $\text{Zn}_5(\text{OH})_8\text{Cl}_2\text{H}_2\text{O}$, $\text{Zn}_{0.71}\text{Al}_{0.29}(\text{OH})_2(\text{CO}_3) \cdot 0.145\text{xH}_2\text{O}$ and $\text{ZnO} \cdot \text{Al}_2\text{O}_3$.

All the corrosion products of the three coatings contained simonkolleite ($\text{Zn}_5(\text{OH})_8\text{Cl}_2\text{H}_2\text{O}$). According to the study of Hosking et al. [13], simonkolleite is a protective layer of corrosion products, almost insoluble in water, but relatively loose on the coating surface.

The study by Friel et al. [14] showed that the amount of ZnO in the pure Zn coating increased during corrosion. Graedel et al. [15] found that ZnO was the main corrosion product produced in the absence of air pollution. Other studies [16] showed that hydrozincite ($Zn_5(CO_3)_2(OH)_6$) was a protective insoluble corrosion product produced by a pure Zn coating. The two carbonate corrosion products produced by a pure Zn coating, $ZnCO_3$ and hydrozincite, were produced by the reaction between $Zn(OH)_2$ and CO_2 in the soil void. The formation rate of the latter was almost instantaneous, and then it was transformed into a porous simonkolleite by a reaction with Cl^- . Fuente et al. [16] showed that the corrosion product layer of a pure Zn coating in a certain environment may appear in two zones: a spongy microcrack outer layer and a relatively dense inner layer. The spongy outer layer was conducive to the entry of O_2 and H_2O , and the inner layer had a relatively strong blocking effect. However, this observation of the microstructure showed that most of the corrosion products were spherical particles. The accumulation of these granular corrosion products led to the appearance of a spongy corrosion product layer, which also indicated that the bond between this product and the coating was not tight and could fall off easily.

The ZnAl alloy coating and ZnAl pseudo-alloy coating first formed a $ZnO \cdot Al_2O_3$ oxide with O_2 in the soil, and then hydration and carbonation reactions generated the ZnAl compound $Zn_{0.71}Al_{0.29}(OH)_2(CO_3)_{0.145} \cdot xH_2O$. The corrosion product of Al was a netlike skeleton structure, which protected loose simonkolleite from falling off, and thus, the further corrosion of the coating by corrosive medium showed a "self-sealing" effect [17].

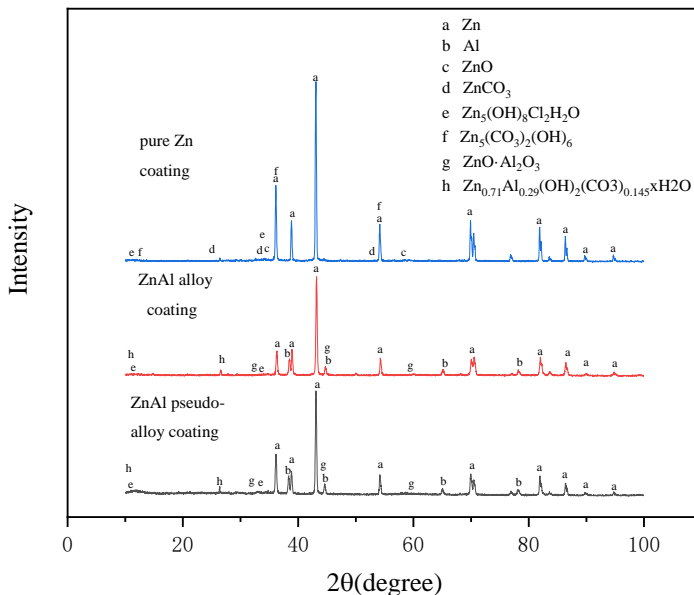


Figure 1. X-ray diffraction patterns of the corrosion products after 120 days of corrosion in soil for the three coatings

3.2 Electrochemical test

Figure 2 shows the polarization curves of the pure Zn, ZnAl alloy and ZnAl pseudo-alloy coating samples after corrosion in soil. The results of the polarization curves after fitting are shown in Table 1.

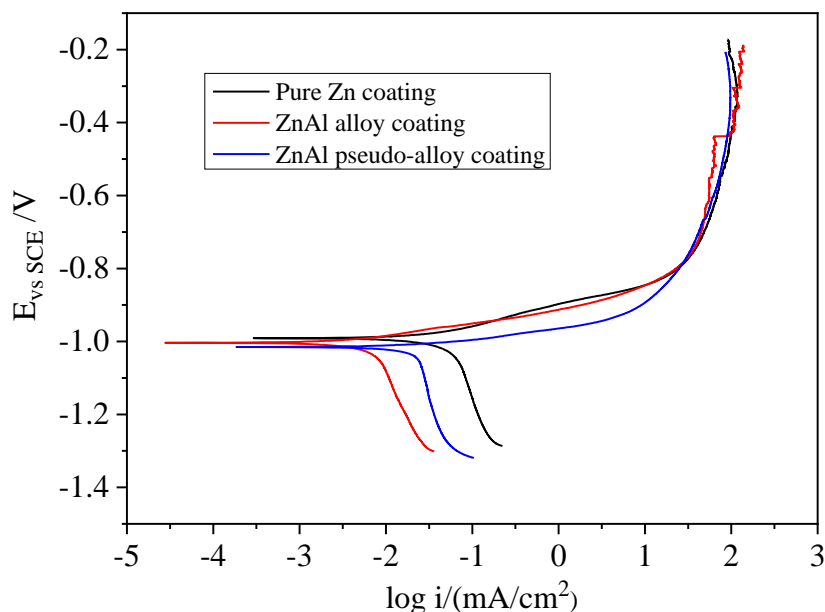


Figure 2. Polarization curves of the three thermal spray coatings in a 3.5 wt% NaCl solution

Table 1. Results of polarization curve fitting for the different coatings

Coating	$E_{\text{corr}}/\text{mV}$	$I_{\text{corr}}/\mu\text{A}$	β_c/mV	β_a/mV
Pure Zn	-990	38.864	718	67
ZnAl alloy	-1003	2.4620	262	33
ZnAl pseudo-alloy	-1014	13.022	996	30

The polarization curve and fitting results are shown in Figure 2. The slope β_c of the Tafel cathode for the three coatings was much higher than the slope β_a of the Tafel anode, which was the cathode control. As shown in Figure 2, there was a diffusion control step on the cathode branch. Since the cathode reaction in the neutral solution may be $\text{O}_2 + 2\text{H}_2\text{O} + 4\text{e} \rightarrow 4\text{OH}^-$, it was the diffusion control step of O_2 . Therefore, the polar diffusion current density of the cathode branch determined the reaction rate. From the anode section of the polarization curve, a relatively dense corrosion product layer was formed on the surface of the coating, which hindered the chemical reaction.

After 120 days of corrosion in soil, the polarization curve fitting results of the three coatings showed that the natural corrosion potential E_{corr} of the pure Zn coating was the highest, followed by the ZnAl alloy coating, and the ZnAl pseudo-alloy coating was the most negative, but the differences were not significant. In addition, it was obvious that the natural corrosion current I_{corr} of the ZnAl alloy coating was far less than that of the other two coatings, among which the I_{corr} of the pure Zn coating was the largest. This indicated that after 120 days of corrosion, the corrosion products produced by the ZnAl alloy coating had the best passivation and self-sealing effects, which reduced the rate of continuous corrosion of the coating.

Figures 3 and 4, show the electrochemical impedance spectra of the three kinds of alloy-coated samples in a 3.5 wt% NaCl solution. A reference to the electrochemical corrosion principle [18], Figure

5 shows the three kinds of coating in front of the corrosion in soil equivalent circuit. Figure 6 shows the pure Zn coating and ZnAl alloy coating in a Beijing area equivalent circuit after corrosion in soil. Figure 7 shows the ZnAl pseudo-alloy coating in a Beijing area equivalent circuit after corrosion in soil, where R_s is the solution resistance, R_r is the resistance for the coating porosity, Q_r is the coating capacitance, R_t is the electrode reaction interface charge transfer resistance, and Q_d is the electric double layer capacitance. According to the equivalent fitting circuits (Figures 5, 6 and 7), the electrochemical impedance spectra of soil samples with three kinds of coating before and after corrosion were fitted, and the results are shown in Tables 2 and 3, respectively.

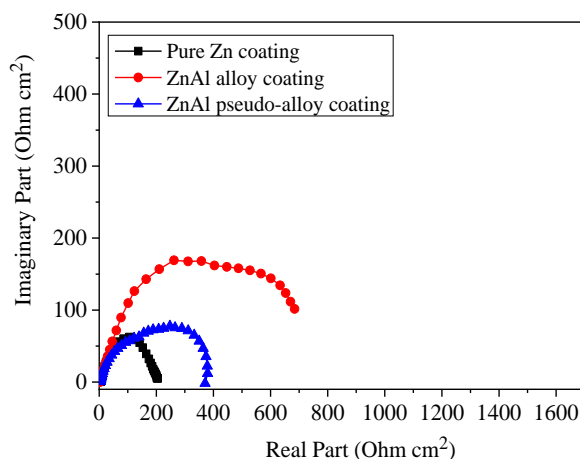


Figure 3. Impedance spectra of the three coatings before corrosion in soil in a 3.5 wt% NaCl solution

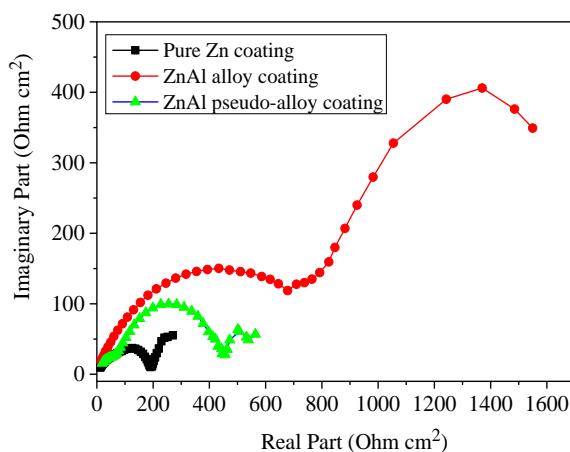


Figure 4. Impedance spectra of the three coatings in 3.5 wt% NaCl solution after 120 days of corrosion in soil in a Beijing area

Due to a dispersion effect, the capacitor element Q was replaced by the constant phase angle element, which was defined as:

$$Z = \frac{1}{Y_0} (j\omega)^{-n}$$

Z — the impedance of Q

j — imaginary part

ω — angular frequency
 Y_0 — constant
 n — diffusion effect index of Q ($0 < n < 1$)

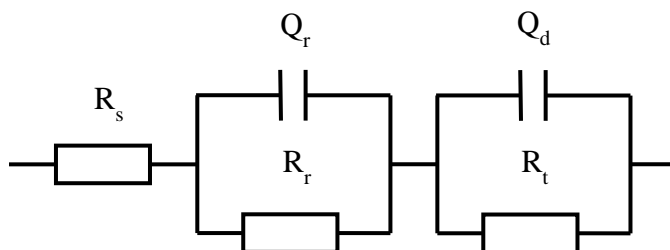


Figure 5. Equivalent circuits of the three original sample coatings before entering a corrosion in soil environment

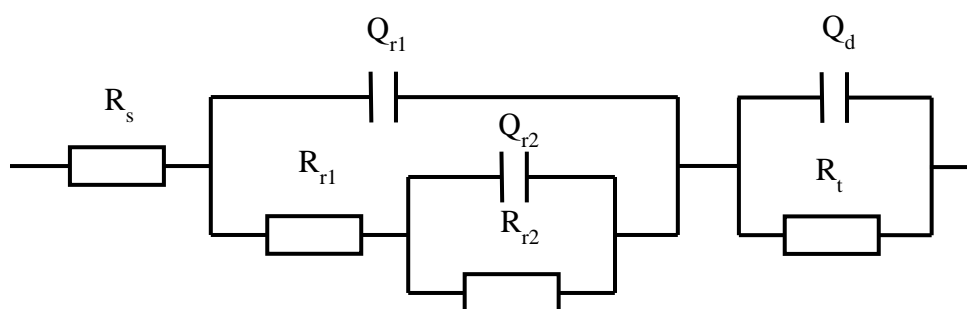


Figure 6. Equivalent circuits of the pure Zn coating and ZnAl alloy coating after 120 days of corrosion in soil in a Beijing area

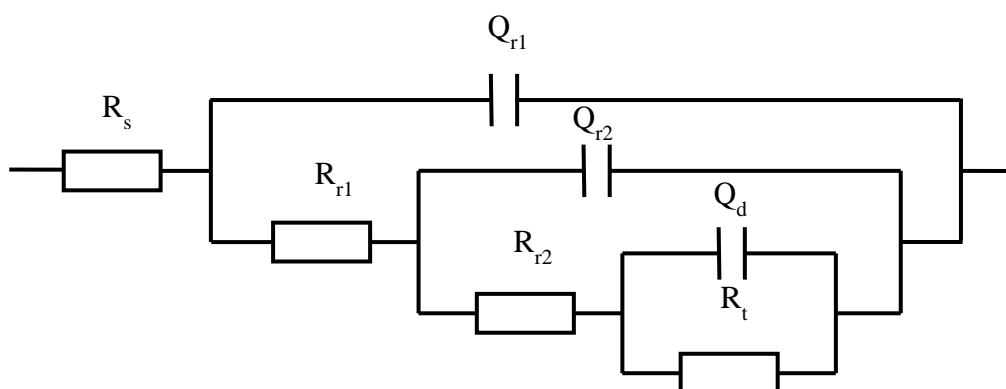


Figure 7. Equivalent circuit of the ZnAl pseudo-alloy coating after 120 days of corrosion in soil in a Beijing area

Table 2. Electrochemical fitting parameters of the three coatings before corrosion in soil

Coating	$R_s/(\Omega \cdot \text{cm}^2)$	$(Y_0)_r/(\Omega^{-1} \cdot \text{cm}^{-2} \cdot \text{S}^{-n_1})$	n_r	$R_r/(\Omega \cdot \text{cm}^2)$	$(Y_0)_d/(\Omega^{-1} \cdot \text{cm}^{-2} \cdot \text{S}^{-n_2})$	n_d	$R_t/(\Omega \cdot \text{cm}^2)$
Pure Zn	3.757	2.923×10^{-2}	0.2782	44.31	1.556×10^{-4}	0.7449	178.20
ZnAl alloy	2.731	5.202×10^{-4}	0.8000	370.00	3.056×10^{-3}	0.8000	4866.00
ZnAl pseudo-alloy	3.079	1.446×10^{-3}	0.8000	277.50	1.874×10^{-4}	0.8000	118.20

Table 3. Electrochemical fitting parameters of the three coatings after corrosion in soil

Coating	$R_s/(\Omega \cdot \text{cm}^2)$	$(Y_0)_{r1}/(\Omega^{-1} \cdot \text{cm}^{-2} \cdot \text{S}^{-n_1})$	n_{r1}	$R_{r1}/(\Omega \cdot \text{cm}^2)$	$(Y_0)_{r1}/(\Omega^{-1} \cdot \text{cm}^{-2} \cdot \text{S}^{-n_1})$	n_{r2}	$R_{r2}/(\Omega \cdot \text{cm}^2)$	$(Y_0)_d/(\Omega^{-1} \cdot \text{cm}^{-2} \cdot \text{S}^{-n_2})$	n_d	$R_t/(\Omega \cdot \text{cm}^2)$
Pure Zn	1.344	6.862×10^{-5}	0.5077	105.30	1.401×10^{-4}	0.6512	90.75	5.524×10^{-2}	0.7696	163.30
ZnAl alloy	0.010	2.383×10^{-5}	0.5997	14.820	2.965×10^{-3}	0.6393	1407.00	7.616×10^{-5}	0.5322	607.50
ZnAl pseudo-alloy	5.024	2.778×10^{-6}	0.7127	61.840	1.033×10^{-4}	0.8530	396.60	3.833×10^{-2}	0.8525	137.20

As shown in Figures 2 and 3, the arc radius of the ZnAl alloy coating was the maximum, and the arc radius of the pure Zn coating was always the minimum. This showed that the three coatings had the ability to resist corrosion in soil and protect the matrix from corrosion at the initial stage, and after 120 days, the order of effectiveness was as follows: ZnAl alloy coatings > ZnAl pseudo-alloy coatings > pure Zn coatings. The diffusion effect index n mainly depended on the inhomogeneity of corrosion current distribution. Y_0 had no effect on the resistance of electrochemical reaction. After 120 days of corrosion, it was obvious that the diffusion effect index n of the ZnAl pseudo-alloy coating was the highest, which indicated that the inhomogeneity of the corrosion current distribution of the coating was the highest.

Figures 5, 6 and 7 show that the equivalent circuits of the three coatings before corrosion in soil are the same and have two time constants. Q_r and R_r reflect the coating state and Q_d and R_t reflect the state at the interface between the coating and the substrate. After 120 days of corrosion in soil, three time constants appeared. Q_{r1} and R_{r1} reflected the state of coating surface corrosion products, Q_{r2} and R_{r2} reflected the state of corrosion in the residual metal and alloy coating, and Q_d and R_t also reflected the state of the coating and substrate interface [18,19]. This was because the three coatings were all thermally sprayed layers, and the coating components before corrosion in soil were all a metal or an alloy without the generation of protective corrosion products. Therefore, two time constants appeared in the equivalent circuit. The three time constants of the equivalent circuit after corrosion in soil indicated that the formation of a corrosion product layer on the outer surface of the coating had an effect on the coating state, which hindered to a certain extent the corrosion of the coating and matrix. Liu et al. [20] showed

that the micro-pores and gaps left by the sprayed coating were evenly distributed in the coating. Contact with a corrosive media in the soil, such as O_2 or Cl^- , caused corrosion reactions to constantly occur on the coating surface, which then formed the corrosion product layer. The difference between the ZnAl pseudo-alloy coating and the equivalent circuits of the pure Zn coating and ZnAl alloy coating was mainly due to the different microstructures. The pure Zn coating and ZnAl alloy coating were single-phase structures with no significant fluctuations for the composition in different regions, while the ZnAl pseudo-alloy coating was composed of Zn-rich and Al-rich phases [4].

Tables 2 and 3 show that the R_s values of the solution resistance for the three coatings were always small before and after corrosion, which showed that the influence of solution resistance on the test results was small. The corrosion resistance of the coatings needed to be analysed by R_t and R_r . The size of R_t reflected the difficulty of the electrochemical reaction at the interface of the matrix. The size of R_r indicated the ability of impeding the penetration of a corrosive medium on the coated metal or corrosion product layer. Both of them explained the corrosion resistance of the coatings as a whole.

The results of Tables 2 and 3 show that the order of the R_t of soil before and after the corrosion test was ZnAl alloy coating > ZnAl pseudo-alloy coating > pure Zn coating. This result showed the electrochemical reaction between the ZnAl alloy coating and its matrix was the most difficult. From another point of view, it was found that chemical reactions in the interface between the coatings with a single-phase structure and its matrix occurred, but the chemical reaction was more difficult than that of coatings with a multi-phase structure. This may be because the phase structure of the coatings with a single-phase structure was relatively homogeneous, and the potential fluctuation between different regions was not large, while the coatings with a multi-phase structure were different due to the phase composition. In addition, the potential difference in the local area was very large, which not only made the coating couple with the matrix but also between the different structures of the coating, thus reducing the difficulty of the electrochemical reaction and reducing the corrosion resistance. The R_t of the pure Zn coating and ZnAl alloy coating decreased before and after corrosion. This may be because there was little or no corrosion medium at the interface between the sample coating and the matrix before corrosion, but after 120 days of corrosion, the external corrosion medium diffused sufficiently from the pore to the matrix interface, which greatly reduced the difficulty of electrochemical reaction at the interface [21]. The reason for the small change in the pure Zn coating and ZnAl pseudo-alloy coating before and after R_t may be that the porosity of the coating was higher than that of the ZnAl alloy; therefore, the penetration of the corrosion medium was higher and the electrochemical reaction at the interface was easier in the process of electrochemical testing of corrosion.

Compared with the R_r in Table 2 and the R_{r2} in Table 3, it was seen that the pore resistance of each coating increased after corrosion in soil, and the increase of the ZnAl alloy coating was most obvious. This was due to the formation of a "self-sealing" structure in the corrosion process of the coating, which included the network skeleton formed by the passivation corrosion products of Al [5,22]. Xing et al. [23] showed that the effect of forming the structure of the ZnAl pseudo-alloy coating was not good, but the pure Zn coating did not have this structure at all and instead the voids were filled by the spongy corrosion products of Zn [24]. Therefore, the pore resistance of the two coatings was much smaller than that of the ZnAl alloy coating, and the corrosion product layer on the surface of the ZnAl alloy coating was thinner, which in a smaller R_{r1} . In addition, the pore resistance of the coating R_r in

Table 2 and R_{r2} in Table 3 was ordered as ZnAl alloy coating > ZnAl pseudo-alloy coating > pure Zn coating, and the R_{r1} of the coating corrosion product resistance in Table 3 was the opposite. This showed that the corrosion product of the pure Zn coating mainly relied on the formation of thicker corrosion products on the surface to protect the matrix during the corrosion in soil stage, El-Mahdy's paper [25] had a similar conclusion. However, the pores of the other two coatings were well blocked by corrosion products, so the matrix was protected in this way. This greatly reduced the corrosion rate of the two coatings and prolonged the service life of the coatings.

Overall, the corrosion resistance of the pure Zn coating was relatively poor, mainly because the corrosion products formed by the coating did not have a role of reinforcement and were easily lost. The reason why the ZnAl pseudo-alloy coating was inferior to the ZnAl alloy coating may be the appearance of Zn-rich phase and Al-rich phase, which resulted in more defects due to the different crystal structure of the two phases in the bonding process and showed an increase in porosity [26]. More importantly, Lowe et al. [27] showed that galvanic corrosion was observed in the experiment. After a period of time, the internal surface or the surface of the coating were damaged to varying degrees, which increased the number of defects and reduced the service life of the coating.

Because the corrosion product simonkolleite produced by Zn was loose and easy fell off [28], there were many cracks and voids [29] on the surface of the pure Zn coating without a "self-sealing" effect; the cracks and voids allowed the corrosive medium access to the inside of the coating, which produced new corrosion products. The corrosion product layer then hindered the diffusion of the corrosive medium. When the corrosion product layer reached a certain thickness, it played a better role in protecting the coating. A pure Zn coating needed to be corroded continuously to maintain the thickness of the corrosion product layer. The composite structure of the ZnAl pseudo-alloy coating increased the defects between the different phases of the coating. In addition, galvanic corrosion formed between the Zn-rich phase and the Al-rich phase, and both factors accelerated the corrosion of coatings. In contrast, the structure of the ZnAl alloy coating was uniform and compact, the pore defects were less than those of the ZnAl pseudo-alloy coating, and the corrosion products of the Al formed a skeletal structure during the corrosion process, which enhanced the "self-sealing" effect. After long-term corrosion in soil, the results showed that the ZnAl alloy coating had a longer service life and a better protective effect.

4. CONCLUSION

(1) The 120-day corrosion in soil test in a Beijing area showed that the corrosion resistance of the ZnAl alloy coating was the best, followed by the pseudo-alloy coating, and then followed by the pure Zn alloy coating, which was the worst based off the polarization curve and electrochemical impedance analysis.

(2) The results of the equivalent circuit fitting showed that the electrochemical reaction between pure Zn coatings and ZnAl alloy coatings with a single-phase structure was more difficult than that of Zn-rich and Al-rich pseudo-alloy coatings.

(3) The self-sealing protective effect of the ZnAl alloy coating was better than that of the ZnAl pseudo-alloy coating because the composition of the ZnAl alloy coating was more uniformly distributed; meanwhile, the pure Zn coating had no self-sealing protective effect.

(4) Because of the existence of Zn-rich and Al-rich phases in the ZnAl pseudo-alloy coating, there were not only many structural defects in the spraying process but also galvanic corrosion between the two phases in the corrosion in soil process. This increased the corrosion rate of the coating to a certain extent. After long-term use, the surface of the ZnAl pseudo-alloy coating showed uneven corrosion with many defects, which shortened the service life of the coating.

ACKNOWLEDGEMENT

This work was supported by the National Key Research and Development Program of China (Grant No. 2017YFB0304602) and the National Environment Corrosion Platform (Grant No. 2005DKA10400).

References

1. Y. Zhang, F. Liu, *Surface and Coatings Technology*, 285 (2016) 235.
2. T. Chen, C. Chou, T. Yung, K. Tsai and J. Huang, *Surface and Coatings Technology*, 303 (2016) 78.
3. R.M. Souto, L. Fernández-Mérida, S. González and D.J. Scantlebury, *Corros. Sci.*, 48 (2006) 1182.
4. K. Bobzin, M. Öte and M.A. Knoch, *Corros. Sci.*, 155 (2019) 217.
5. A.R. Marder, *Progress in Materials Science*, 45 (2000) 191.
6. S. Djerourou, H. Lahmar and N. Bouhellal, *Advanced materials research*, 685 (2013) 271.
7. A.R. Trueman, *Corros. Sci.*, 47 (2005) 2240.
8. K. Bobzin, M. Öte, M.A. , *Journal of Thermal Spray Technology*, 26 (2017) 464.
9. H. Katayama, S. Kuroda, *Corros. Sci.*, 76 (2013) 35.
10. R.M. Kain and E.A. Baker , *Testing of Metallic & Inorganic Coatings*, (1987).
11. Y. Liu, Z. Zhu and Y. Chen, *China Surface Engineering*, 14 (2004) 443.
12. M. Zhu, C. Du and X. Li , *Journal of Chinese Society for Corrosion and Protection*, 33 (2013) 306.
13. N.C. Hosking, M.A. Strom, P.H. Shipway and C.D. Rudd, *Corros. Sci.*, 49 (2007) 3669.
14. J.J. Friel, *Corrosion*, 42 (1986) 422.
15. T.E. Graedel, *Electrochem. Soc.*, 136 (1989) 193.
16. D. D. Fuente, J.G. Castano and M. Morcillo, *Corros. Sci.*, 49 (2007) 1420.
17. M.K. Lei, X.P. Zhu, K.W. Xu and B.S. Xu, *Key Engineering Materials*, 373 (2008) 64.
18. C. Cao, *The corrosion electrochemistry principle*, (2004) 55.
19. L. Li, P. Qiu and X. Su, *Corros. Prot.*, 35 (2014) 845.
20. A. Liu, K. Xiao, X. Li and J. Yuan, *Thermal Spray Technology*, 7 (2015) 46.
21. Y. Xiao, X. Jiang, Y. Xiao and L. Ma, *Procedia Engineering*, 27 (2012) 1644.
22. P.R. Seré, M. Zapponi, C. Elsner and A.D. Sarli, *Corros. Sci.*, 40 (1998) 1711.
23. S. Xing, K. Xiao, L. Li, A. Liu, X. Li and C. Dong, *Corros. Prot.*, 33 (2012) 236.
24. Q. Jing, Q. Miao, X. Ding and X. Wei, *Mater. Prot.*, 45 (2012) 51.80
25. G.A. El-Mahdy, A. Nishikata and T. Tsuru, *Corros. Sci.*, 42 (2000) 1509.
26. M. Bütetführ, *Mater. Corros.*, 9 (2007) 721.
27. T.A. Lowe, G.G. Wallace and A.K. Neufeld, *Journal of Solid State Electrochemistry*, 13 (2009) 619.
28. Y. Li, *Corros. Sci.*, 43 (2001) 1793.
29. A. Liu, K. Xiao, C. Fang, E. Wang, D. Wei, J. Gao and X. Li, *Mater. Prot.*, 44 (2011) 12.